



Title	Second-harmonic dielectric response of an antiferroelectric liquid crystal under dc electric fields
Author(s)	Fajar, Andika; Orihara, Hiroshi
Citation	Physical Review E, 81(3), 031710 https://doi.org/10.1103/PhysRevE.81.031710
Issue Date	2010-03
Doc URL	http://hdl.handle.net/2115/43005
Rights	©2010 The American Physical Society
Type	article
File Information	PRE81-3_031710.pdf



[Instructions for use](#)

Second-harmonic dielectric response of an antiferroelectric liquid crystal under dc electric fields

Andika Fajar

PTBIN-BATAN, Kawasan Puspiptek Serpong, Tangerang 15314, Indonesia

Hiroshi Orihara

Department of Applied Physics, Hokkaido University, Sapporo 060-8628, Japan

(Received 9 October 2009; published 24 March 2010)

Second-harmonic dielectric response under dc fields in an antiferroelectric liquid-crystal 4-(1-methyl-heptyloxycarbonyl)phenyl 4-octylcarbonyloxybiphenyl-4-carboxylate (MHPOCBC) has been investigated. The second-harmonic response from the amplitude mode in the smectic- C_α^* phase was observed due to the symmetry breaking by the application of dc electric fields. A Landau theory was developed in order to analyze experimentally obtained frequency dispersions. From the analysis we found a softening of the amplitude mode with increasing the dc field at a temperature close to the smectic- C_α^* -smectic- A phase transition point. It was turned out that the relaxation frequency of the amplitude mode decreases linearly with the applied electric field.

DOI: [10.1103/PhysRevE.81.031710](https://doi.org/10.1103/PhysRevE.81.031710)

PACS number(s): 61.30.-v, 64.70.M-, 77.22.Gm

I. INTRODUCTION

The response of dielectrics to an external electric field has been extensively investigated in order to clarify the phenomena related to structural phase transitions in ferroelectric and antiferroelectric liquid crystals. However, the investigation was mainly confined to the linear response, which is proportional to the applied field. It can only detect modes which induce macroscopic polarizations such as the ferroelectric mode (the tilting fluctuation of the director toward the direction perpendicular to the field) and the ferroelectric Goldstone mode (the azimuthal fluctuation of the director around the helical axis) [1–7]. Recently, on the other hand, the nonlinear dielectric spectroscopy has been shown to become a powerful tool to investigate nonpolar modes related to nonferroelectric phase transitions, which are not observable with the linear one [8–16]. Most of the nonlinear dielectric measurements were performed without applying dc electric fields. As in solid ferroelectrics, applying an electric field is a good method to investigate the dielectric properties. Hereafter, we briefly explain the third-order dielectric spectroscopy under dc electric fields.

In general, the electric displacement $D(t)$ can be expressed in terms of the electric field $E(t)$ as

$$D(t) = \int_{-\infty}^t d\tau_1 \varepsilon_1(t - \tau_1) E(\tau_1) + \int_{-\infty}^t d\tau_1 \int_{-\infty}^{\tau_1} d\tau_2 \int_{-\infty}^{\tau_2} d\tau_3 \times \varepsilon_3(t - \tau_1, t - \tau_2, t - \tau_3) E(\tau_1) E(\tau_2) E(\tau_3) + \dots, \quad (1)$$

where $\varepsilon_1(t_1)$ is the linear after-effect function and $\varepsilon_3(t_1, t_2, t_3)$ is the third-order multiple time after-effect function with a symmetric property with respect to the permutation of the time variables (t_1, t_2, t_3) , which characterizes the nonlinear response. Here we have assumed that the dielectrics considered here is nonpolar, which is the case for the sample used in our experiment. When we apply an electric field such as $E(t) = E_{DC} + E_0 \cos \omega t$, Eq. (1) yields

$$D(t) = D_0 + \text{Re}[D_1(\omega) \exp(i\omega t) + D_2(\omega) \exp(i2\omega t) + D_3(\omega) \exp(i3\omega t) + \dots], \quad (2)$$

with

$$D_0(\omega) = \varepsilon_1(0) E_{dc} + \dots, \quad (3a)$$

$$D_1(\omega) = \text{Re}[\{\varepsilon_1(\omega) E_0 + 3\varepsilon_3(0, 0, \omega) E_{DC}^2 E_0 + \dots\} \times \exp(i\omega t)], \quad (3b)$$

$$D_2(\omega) = \text{Re} \left[\left\{ \frac{3}{2} \varepsilon_3(0, \omega, \omega) E_{DC} E_0^2 + \dots \right\} \times \exp(i2\omega t) \right], \quad (3c)$$

$$D_3(\omega) = \text{Re} \left[\left\{ \frac{1}{4} \varepsilon_3(\omega, \omega, \omega) E_0^3 + \dots \right\} \times \exp(i3\omega t) \right], \quad (3d)$$

where $\varepsilon_1(\omega_1)$ and $\varepsilon_3(\omega_1, \omega_2, \omega_3)$ are defined as

$$\varepsilon_1(\omega_1) \equiv \int_0^\infty d\tau_1 \varepsilon_1(\tau_1) \exp[-i\omega_1 \tau_1], \quad (4a)$$

$$\varepsilon_3(\omega_1, \omega_2, \omega_3) \equiv \int_0^\infty d\tau_1 \int_0^\infty d\tau_2 \int_0^\infty d\tau_3 \varepsilon_3(\tau_1, \tau_2, \tau_3) \times \exp[-i(\omega_1 \tau_1 + \omega_2 \tau_2 + \omega_3 \tau_3)]. \quad (4b)$$

As is seen from Eq. (3), the third-order term in Eq. (1) generates the fundamental, second, and third harmonics under the dc electric field. Note that they are all the third-order responses with respect to the electric field. Without dc electric field, $\varepsilon_3(\omega, \omega, \omega)$ has been measured in an antiferroelectric liquid-crystal MHPOCBC, and the soft and amplitude modes related to the smectic- A (Sm- A)-smectic- C_α^* (Sm- C_α^*) phase transition were successfully observed [14,15]. In addition, the antiferroelectric Goldstone mode was also observed in the antiferroelectric phase, smectic- C_A^* (Sm- C_A^*), of 4-(1-methyl-heptyloxycarbonyl) phenyl 4-octylbiphenyl-4-

carboxylate (MHPOBC) and 4-(1-trifluoromethylheptyloxycarbonyl) phenyl 4-octylbiphenyl-4-carboxylate (TFMHPOBC) [10,11]. As for $\varepsilon_3(0,0,\omega)$, it was measured in the Sm- C_α^* phase of MHPOBC. Bourny *et al.* [17] investigated the dc field dependence of the linear dielectric constant near the Sm-A–Sm- C_α^* phase transition point and observed the amplitude mode in Sm- C_α^* phase. In this experiment, dc bias field (E_{DC}) was changed from 0 to 1.2 V/ μm , while the probe field (E_0) was 0.004 V/ μm . Therefore, at large E_{dc} higher-order nonlinear contributions to the term of $E_{dc}^2 E_0 \exp(i\omega t)$ in $D(t)$ may become large so that the coefficient may deviate from $3\varepsilon_3(0,0,\omega)$. In their analysis, however, the higher-order nonlinearity was considered. It is needless to say that the definition of the above nonlinear dielectric constants is valid only for small E_{dc} and E_0 .

Until now there is no report on $\varepsilon_3(0,\omega,\omega)$ for studying the dynamic properties in smectic liquid crystals and even in solid ferroelectrics. In general, the second-harmonic response is absent for nonpolar dielectrics. But when subjected to an external field it can appear due to the symmetry breaking. This paper will report the emergence of the second-harmonic response under dc fields in an antiferroelectric liquid-crystal MHPOBC. In order to analyze the experimentally observed frequency dispersions we derived the expression for $\varepsilon_3(0,\omega,\omega)$ in the Sm- C_α^* phase from the phenomenological theory as given in the next section. From the simultaneous measurements of fundamental and second-harmonic response and using the theory we describe the behavior of relaxation modes under dc fields close to the Sm- C_α^* –Sm- C phase transition, particularly the amplitude mode which is not reported yet.

II. THEORY

We can derive the expression for $\varepsilon_3(0,\omega,\omega)$ from the phenomenological theory used for $\varepsilon_3(\omega,\omega,\omega)$ in the Sm- C_α^* phase as mentioned in our previous papers [14,15]. The derivation is almost the same; the applied electric field is $E(t) = E_{DC} + E_0 \cos \omega t$ for the former, while $E(t) = E_0 \cos \omega t$ for the latter. Hereafter, we will not repeat the derivation but only show the results.

The linear dielectric constant $\varepsilon_1(\omega)$ and the third-order dielectric for the second-order harmonic $\varepsilon_3(0,\omega,\omega)$ are, respectively, given as

$$\varepsilon_1(\omega) = \chi_f + \varepsilon_\perp + \frac{\varepsilon_a}{2} \xi_s^2 + \chi_f^2 \lambda_f^2 \chi_f(\omega), \quad (5a)$$

$$\begin{aligned} \varepsilon_3(0,\omega,\omega) = & \frac{8}{3} \xi_s^2 [2c(2\omega,\omega)c(0,\omega)\chi_a(\omega) \\ & + c(2\omega,0)c(\omega,\omega)\chi_a(2\omega)] \\ & + b_f \chi_f^3 \lambda_f^3 \chi_f(2\omega)\chi_f(\omega)\chi_f(0). \end{aligned} \quad (5b)$$

with

$$\chi_a(\omega) = (\tilde{a} + i\omega\gamma_a)^{-1}, \quad (6a)$$

$$\chi_f(\omega) = (\tilde{a}_f + i\omega\gamma_f)^{-1}, \quad (6b)$$

$$c(\omega_1,\omega_2) = \frac{\varepsilon_a}{4} - \frac{1}{2} \eta \chi_f^2 \lambda_f^2 \chi_f(\omega_1)\chi_f(\omega_2), \quad (7)$$

where $\chi_a(\omega)$ and $\chi_f(\omega)$ are, respectively, the susceptibilities of the amplitude mode and the ferroelectric mode, and the parameters such as \tilde{a} , \tilde{a}_f , etc., which appear in the free energy, should be referred to Refs. [14,15]. Furthermore, ξ_s is the spontaneous tilt angle, ε_\perp and ε_a are, respectively, the dielectric constant perpendicular to molecules and the dielectric anisotropy, γ_a and γ_f are, respectively, the viscosity coefficients of the amplitude and ferroelectric modes. The amplitude mode modifies the tilt angle in the same way in each smectic layer, producing no polarization, while the ferroelectric mode induces polarization. Therefore, the latter is detectable by the linear dielectric measurement as is seen from Eq. (5a), but the former is not. From Eq. (5b), however, the amplitude mode can be observed by the second-harmonic dielectric response. The first term of the right-hand side in Eq. (5b) originates in the amplitude mode and is a linear function of the susceptibilities of the amplitude mode for ω and 2ω , $\chi_a(\omega)$ and $\chi_a(2\omega)$.

III. EXPERIMENTAL

The sample used in the present experiment was MHPOBC. The phase sequence of MHPOBC without electric field is Sm-A (105.5 °C) Sm- C_α^* (99.5 °C) Sm- C_A^* . The experimental results presented here were all performed in commercially available cells (EHC). The cell gap was about 25 μm , and the area of electrodes with ITO (indium tin oxide) and polyimide alignment layers was $4 \times 4 \text{ mm}^2$. The sample was introduced into a cell in the isotropic phase and it was cooled down slowly to the Sm-A phase. The sample cell was mounted on a hot stage (Instec HS1).

Regarding the nonlinear experiments, there is no device commercially available for measurements of the nonlinear dielectric constants at various frequencies. In general, the nonlinear response is much smaller than the linear one so that a precise measurement of nonlinear response is difficult to be done. In order to overcome this difficulty, a new measurement system was developed. The homemade measurement system of nonlinear dielectric constant was described in detail in the previous work [15]. This system utilizes the vector signal analyzer (HP89410A) which allows one to obtain the amplitudes and the phases of the fundamental, second-, and the third-harmonic dielectric responses simultaneously. The frequency dispersions in all phases of the sample were measured from 100 Hz to 1 MHz at stabilized temperatures on cooling process with a step of 0.5 °C. The driving ac electric field was kept at 0.28 V/ μm . Since the limitation of the equipment, the dc field was applied up to 0.64 V/ μm .

IV. DISCUSSION

Figure 1 shows the temperature dependences of the real parts of $D_1(\omega)$ without dc field and $D_2(\omega)$ with dc fields of 0 and 0.36 V/ μm , measured at 1 kHz. Note that from Eq. (3), $D_1(\omega)$ without dc field is proportional to the linear dielectric

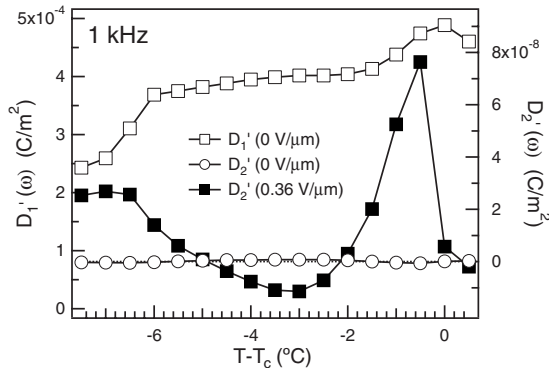


FIG. 1. Temperature dependences of the real parts of $D_1(\omega)$ and $D_2(\omega)$ measured simultaneously on cooling process at the frequency of 1 kHz. T_c indicates the transition point from the Sm-A phase to Sm- C_α^* phase as decreasing the temperature.

constant, $\epsilon_1(\omega)$. Three temperature regions are recognized, corresponding to the paraelectric Sm-A, Sm- C_α^* and antiferroelectric Sm- C_A^* phases. The transition temperature between the Sm-A and Sm- C_α^* phases, T_c , is identified from the peak of the linear dielectric constant [15]. The transition from Sm- C_α^* phase to the Sm- C_A^* phase is recognized as a steep decrease in the linear dielectric constant at about $T-T_c = -6^\circ\text{C}$.

The linear dielectric constant increases gradually in the Sm-A phase as the transition point is approached and takes a maximum, and then it decreases in the Sm- C_α^* phase as has been reported by Isozaki *et al.* [18]. The linear dielectric constant is proportional to the susceptibility of the ferroelectric mode, $\chi_f(\omega)$ [15]. Therefore, this gradual increase with decreasing temperature in the Sm-A phase indicates the partial softening of the ferroelectric mode.

As for the second-harmonic response $D_2(\omega)$, on the other hand, it strongly depends on the dc field. Without dc field, a very small response was observed in the measurement. In all the phases, Sm-A, Sm- C_α^* , and Sm- C_A^* , $+x$ and $-x$ directions are identical so that the second-harmonic response should vanish from the symmetry. The small response may come from the surface effect or defects, which can bring about the symmetry breaking. While in the presence of dc field, the response becomes large and shows a complicated temperature dependence. In the Sm- C_α^* phase it increases steeply and takes a peak just below the transition temperature and then decrease with decreasing the temperature. At 2°C below the transition point, the value becomes zero and the sign changes to negative. With further decreasing temperature, the sign changes from negative to positive near the transition point to Sm- C_A^* phase. This temperature dependence of the second-harmonic response under dc field is almost the same as the third-harmonic dielectric response without dc field [15]. This is natural because the second-harmonic response with dc electric field and the third-harmonic one, $\epsilon_3(\omega, \omega, \omega)$, without dc electric field are both a linear function of the linear susceptibility of the amplitude mode, which may have the dominant temperature dependence.

Next, the typical frequency dispersions of the fundamental, second-, and third-harmonic dielectric responses at $T-T_c = -0.5^\circ\text{C}$ in the Sm- C_α^* phase are shown in Fig. 2 with-

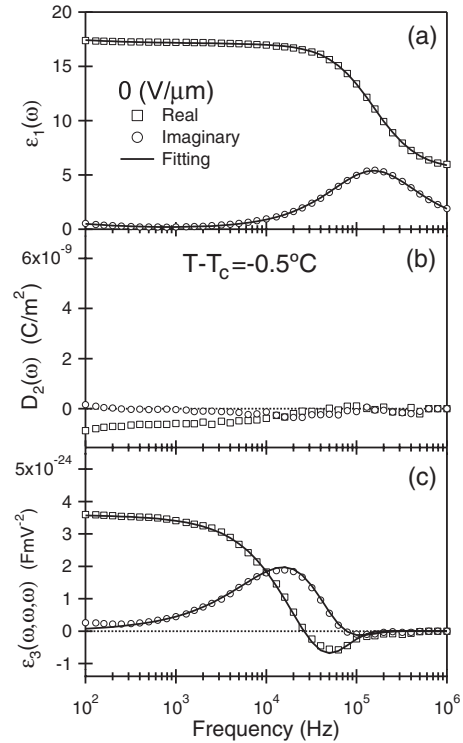


FIG. 2. Typical frequency dispersions of (a) $\epsilon_1(\omega)$, (b) $D_2(\omega)$, and (c) $\epsilon_3(\omega, \omega, \omega)$ obtained at $T-T_c = -0.5^\circ\text{C}$ in the Sm- C_α^* phase at zero dc field.

out dc field and in Fig. 3 with dc field. It is seen from Figs. 2(a) and 3(a) that only one Debye-type relaxation mode, which is a homogeneously tilting mode, i.e., the ferroelectric mode, is involved in the linear dielectric constant in the measured frequency region. A slight increase in dielectric constant at low frequencies should be due to ionic conduction.

As for the second-harmonic response, it is almost zero without dc electric field as shown in Fig. 2(b). Note that in Fig. 2(b) $D_2(\omega)$ is shown instead of $\epsilon_3(0, \omega, \omega)$ because of zero dc electric field. While in the presence of dc electric field [Fig. 3(b)], we obtained a dispersion different from that of the linear one. This dispersion is similar to the third-harmonic ones without dc field [Fig. 2(c)] and with dc field [Fig. 3(c)], indicating that both the second- and third-harmonic responses originate in the linear susceptibility of the amplitude mode, as was theoretically predicted. At the limit of $\omega \rightarrow 0$, $\epsilon_3(\omega, \omega, \omega)$ and $\epsilon_3(0, \omega, \omega)$ should be the same. They are almost the same as shown in Figs. 3(b) and 3(c). The discrepancy may come from the higher-order nonlinearities.

In our previous paper [15], the expression for $\epsilon_3(\omega, \omega, \omega)$ under zero dc field in the Sm- C_α^* phase was derived to obtain the relaxation frequency of the amplitude mode from experimentally obtained frequency dispersions. The amplitude mode was confirmed to become soft near the transition point. The solid lines in Figs. 2(c) and 3(c) are obtained by the fittings. Here, let us fit the dispersion curve in Fig. 3(b) to Eq. (5b) in order to compare the relaxation frequencies obtained from the second and third harmonics. Using Eqs. (6a), (6b), and (7), Eq. (5b) is rewritten as

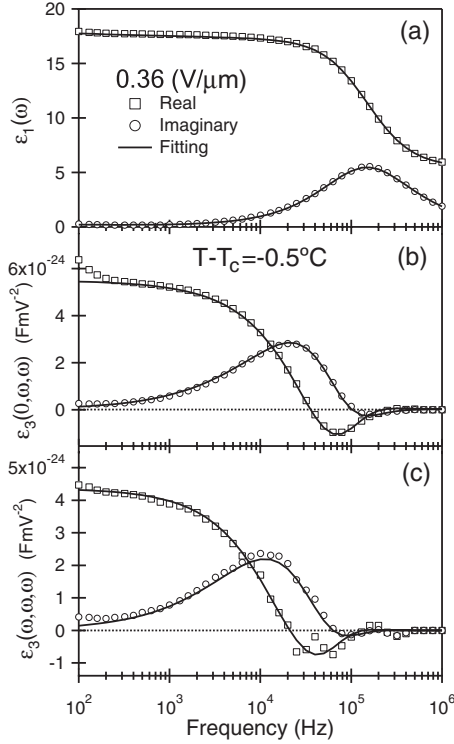


FIG. 3. Typical frequency dispersions of (a) $\epsilon_1(\omega)$, (b) $\epsilon_3(0, \omega, \omega)$, and (c) $\epsilon_3(\omega, \omega, \omega)$ obtained at $T - T_c = -0.5$ °C in the Sm-C_α^* phase at a dc field of 0.36 $\text{V}/\mu\text{m}$.

$$\begin{aligned} \epsilon_3(0, \omega, \omega) = & \frac{A_{a1}}{1 + (i\omega\tau_a)^{\beta_a}} \left(1 - \frac{p}{(1 + i2\omega\tau_f)(1 + i\omega\tau_f)} \right) \\ & \times \left(1 - \frac{p}{1 + i\omega\tau_f} \right) + \frac{A_{a2}}{1 + (i2\omega\tau_a)^{\beta_a}} \\ & \times \left(1 - \frac{p}{1 + i2\omega\tau_f} \right) \left(1 - \frac{p}{(1 + i\omega\tau_f)^2} \right) \\ & - \frac{A_f}{(1 + i2\omega\tau_f)(1 + i\omega\tau_f)}, \end{aligned} \quad (8)$$

where τ_a and τ_f are the relaxation times of the amplitude and ferroelectric modes, respectively. A distribution parameter β_a has been introduced. There were many adjustable parameters so that we first determined τ_f from the linear dielectric dispersion in Fig. 3(a) by using the following equation:

$$\epsilon_1(\omega) = \epsilon_\infty + \frac{\Delta\chi_f}{1 + (i\omega\tau_f)^{\beta_f}} + \frac{1}{(i\omega\tau_i)^\delta}, \quad (9)$$

where the last term has been added to take the conductivity into account, and ϵ_∞ is the dielectric constant at the high frequency limit, $\Delta\chi_f$ is the dielectric strength, and β_f and δ are distribution parameters. The fitting results using the least-squares method are shown by solid lines in Fig. 3(a). The linear dielectric dispersion is well fitted to Eq. (9), and the distribution parameter β_f was almost 1. The second-harmonic dielectric response is also reproduced by Eq. (8) except at low frequencies, where the ionic conduction becomes large. The relaxation frequencies of the amplitude

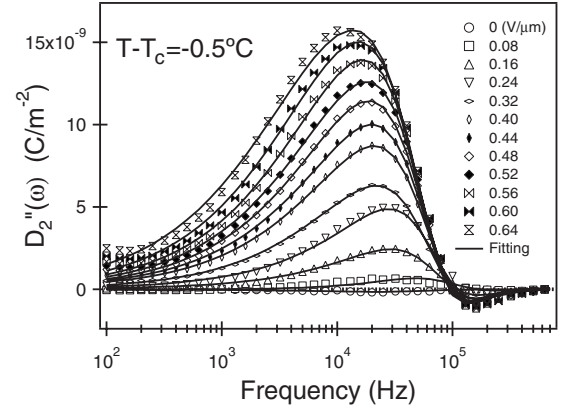


FIG. 4. Dependence of the imaginary part of $D_2''(\omega)$ on dc field at $T - T_c = -0.5$ °C (Sm-C_α^*).

mode, $(2\pi\tau_a)^{-1}$, obtained from Figs. 2(c) and 3(b) are, respectively, 38 and 31 kHz, which are in good agreement.

The frequency dispersions of $D_2''(\omega)$ at different dc electric fields in the raising process of the field measured at $T - T_c = -0.5$ °C was shown in Fig. 4. As mentioned above, a very small second-harmonic dielectric response was observed at zero dc field, and the strength becomes larger with increasing the dc field. It was reported that at large dc fields the Sm-C_α^* phase is changed into Sm-C [17]. However, in the present experiment the field-induced phase transition was not attained because of the limitation of our measurement system. From Fig. 4 it is clearly seen that the peak frequency shifts to lower frequencies with increasing the dc field.

Analysis using Eq. (8) are valid only for small E_{dc} and E_0 . In our experiments E_{DC} was increased to considerably large values. However, we may be able to obtain an approximate value of τ_a . The solid lines in Fig. 4 are fitted results. Figure 5 shows the dc field dependences of the relaxation frequencies of the ferroelectric mode and the amplitude mode, $f_{r,f} = (2\pi\tau_f)^{-1}$ and $f_{r,a} = (2\pi\tau_a)^{-1}$, obtained from the fitting. The relaxation frequency of the amplitude mode, $f_{r,a}$, decreases with increasing the dc field. It seems to become zero toward the field-induced transition point from Sm-C_α^* to Sm-C

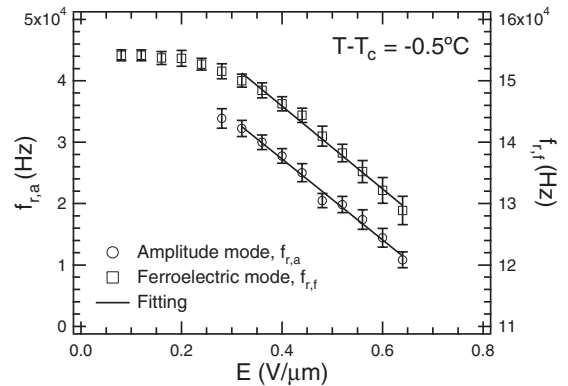


FIG. 5. Dc field dependences of the relaxation frequencies obtained from the linear and the second-order nonlinear dielectric spectroscopies. $f_{r,f}$ and $f_{r,a}$ are the relaxation frequencies of the ferroelectric mode obtained from the fitting result using Eq. (9) and the amplitude mode using Eq. (8), respectively.

around $0.81 \text{ V}/\mu\text{m}$, namely, the softening of amplitude mode takes place. In the high dc field region, the Curie-Weiss law with respect to the dc electric field holds for this mode. For the ferroelectric mode, on the other hand, partial softening is seen.

We notice an interesting fact that the slopes of the amplitude $[-65.9 \pm 2.4 \text{ kHz}/(\text{V}/\mu\text{m})]$ and ferroelectric $[-67.4 \pm 2.5 \text{ kHz}/(\text{V}/\mu\text{m})]$ modes are almost the same. A similar result was obtained in the temperature dependences of the relaxation frequencies of the soft and ferroelectric modes in the Sm-A phase [15]. The temperature dependence was explained in terms of a discrete model [19], but the field dependence is not yet clarified at present.

V. CONCLUSIONS

The second-harmonic dielectric measurements under dc fields have been performed in the Sm- C_a^* phase. The second-harmonic dielectric response did not exist at zero dc field, while in the presence of dc electric field it emerged due to the symmetry breaking. We developed a phenomenological theory and obtained the expression for the second-harmonic dielectric response under dc electric fields, $\epsilon_3(0, \omega, \omega)$, which turned out to be a linear function of the linear susceptibility of the amplitude mode as well as the third-harmonic response, $\epsilon_3(\omega, \omega, \omega)$. From the analysis of the obtained frequency dispersions, it was found that a softening of amplitude mode takes place and in the high dc field region the

Curie-Weiss law with respect to dc electric field holds for this mode. On the other hand, a partial softening was seen for the ferroelectric mode. The slopes of the field dependences of the amplitude and ferroelectric modes are almost the same. Theoretical considerations based on the discrete model will be necessary to clarify the dc field dependence of the modes. At the end of this paper, we would like to emphasize that the second-harmonic generation (SHG) is very sensitive to the symmetry change from nonpolar to polar states, as clearly shown in Figs. 1 and 4. In the present paper the symmetry change was caused by applying dc electric fields, however SHG measurements will make it possible to observe symmetry changes brought about not only by the dc-bias electric fields but also by the other causes such as the presence of defects. The optical SHG measurement is widely used for detecting them, but the dielectric one is not yet. Since the latter has an additional advantage that it can easily give frequency dispersions, we believe it will become a powerful tool.

ACKNOWLEDGMENTS

We would like to thank Showa Shell Sekiyu Co. Ltd. for supplying MHPOCBC. This work was supported by KAKENHI (Grant-in-Aid for Scientific Research) on Priority Area "Soft Matter Physics" and Scientific Research (C) (Grant No. 19540326) from the Ministry of Education, Culture, Sports, Science and Technology of Japan.

-
- [1] M. Ozaki, T. Hatai, and K. Yoshino, *Jpn. J. Appl. Phys., Part 2* **27**, L1996 (1988).
- [2] C. Bahr and G. Heppke, *Phys. Rev. A* **39**, 5459 (1989).
- [3] T. Fujikawa, H. Orihara, Y. Ishibashi, Y. Yamada, N. Yamamoto, K. Mori, K. Nakamura, Y. Suzuki, T. Hagiwara, and I. Kawamura, *Jpn. J. Appl. Phys., Part 1* **30**, 2826 (1991).
- [4] S. K. Kundu, E. Okabe, W. Haase, and B. K. Chaudhuri, *Phys. Rev. E* **64**, 051708 (2001).
- [5] R. Douali, C. Legrand, V. Laux, N. Isaert, G. Joly, and H. T. Nguyen, *Phys. Rev. E* **69**, 031709 (2004).
- [6] Z. Kutnjak, *Phys. Rev. E* **70**, 061704 (2004).
- [7] J. Hemine, C. Legrand, A. Daoudi, N. Isaert, A. Elkaouachi, and H. T. Nguyen, *J. Phys.: Condens. Matter* **19**, 296203 (2007).
- [8] H. Orihara, H. Mizuno, M. Iwata, and Y. Ishibashi, *Mol. Cryst. Liq. Cryst.* **328**, 265 (1999).
- [9] H. Orihara, A. Fukase, and Y. Ishibashi, *J. Phys. Soc. Jpn.* **64**, 976 (1995).
- [10] K. Obayashi, H. Orihara, and Y. Ishibashi, *J. Phys. Soc. Jpn.* **64**, 3188 (1995).
- [11] Y. Kimura, R. Hayakawa, N. Okabe, and Y. Suzuki, *Phys. Rev. E* **53**, 6080 (1996).
- [12] H. Murai, V. Bourny, A. Fajar, and H. Orihara, *Mol. Cryst. Liq. Cryst. Sci. Technol., Sect. A* **366**, 645 (2001).
- [13] Y. Kimura, H. Isono, and R. Hayakawa, *Eur. Phys. J. E* **9**, 3 (2002).
- [14] H. Orihara, A. Fajar, and V. Bourny, *Phys. Rev. E* **65**, 040701(R) (2002).
- [15] A. Fajar, H. Murai, and H. Orihara, *Phys. Rev. E* **65**, 041704 (2002).
- [16] A. Fajar and H. Orihara, *Mol. Cryst. Liq. Cryst.* **511**, 239 (2009).
- [17] V. Bourny and H. Orihara, *Phys. Rev. E* **63**, 021703 (2001).
- [18] T. Isozaki, Y. Suzuki, I. Kawamura, K. Mori, N. Nakamura, N. Yamamoto, Y. Yamada, H. Orihara, and Y. Ishibashi, *Jpn. J. Appl. Phys., Part 2* **30**, L1573 (1991).
- [19] H. Sun, H. Orihara, and Y. Ishibashi, *J. Phys. Soc. Jpn.* **62**, 2706 (1993).